TÜBİTAK

Turkish Journal of Earth Sciences

http://journals.tubitak.gov.tr/earth/

Research Article

Turkish J Earth Sci
(2013) 22: 1033-1046

doi:10.3906/yer-1210-10

Investigation of the groundwater effect on slow-motion landslides by using dynamic Kalman filtering method with GPS: Koyulhisar town center

Kemal Özgür HASTAOĞLU*
Department of Geomatics Engineering, Division of Geodesy, Faculty of Engineering, Cumhuriyet University, Sivas, Turkey

Received: 30.10.2012 • **Accepted:** 06.07.2013 • **Published Online:** 11.10.2013 • **Printed:** 08.11.2013

Abstract: The monitoring and analysis of natural disasters and their systems is crucially important in minimizing loss of life and property. In recent years, various methods of measurement and analysis have been employed to monitor and analyze landslides and their mechanisms. The Global Positioning System (GPS) is one of the methods used to monitor landslides. The consideration of external forces causing movement is essential when interpreting movement obtained by GPS. This paper describes a large motion in the Koyulhisar town center obtained from one GPS point. Twelve GPS points were set up in the Koyulhisar landslide region; 6 periods of GPS measurements were performed. The resultant data were processed using Bernese V5.0 software and coordinate information related to the points was obtained. In this study, the relationship between large motion and external forces was mathematically determined in a different way from previous studies. The coordinate information was first analyzed using the kinematic Kalman filtering technique and time-dependent speed and acceleration values for the points were determined. Data from the points at which significant displacements were observed were then analyzed using the dynamic Kalman filtering technique and the relationship between significant movements and temperature was modeled. Finally, the dynamic and kinematic model results were compared; it was observed that the displacements predicted by the dynamic model were more consistent with real values. It is concluded that accuracy in developing prediction models for deformations in landslides would be improved by using a dynamic deformation model containing either forces causing deformations or functions of quantities related to these forces.

Key words: Landslide monitoring, dynamic Kalman filtering, GPS

1. Introduction

A detailed analysis of landslide motion necessitates the determination of positions of Global Positioning System (GPS) points in 3 dimensions (Dercourt 2000; Malet *et al.* 2002). GPS systems determine 3-dimensional point positions, with precision in millimeters, by using phase measurements. This precision allows GPS systems to be easily utilized in monitoring landslides. The literature contains a number of studies related to the monitoring of landslides (Brunner 1993, 1997; Dercourt 2000; Gili *et al.* 2000; Malet *et al.* 2002; Bayrak 2003; Coe *et al.* 2003). Particularly, it is necessary to produce results using a suitable analysis method and a deformation model in order to analyze landslide mechanisms and determine movement amounts using GPS.

In periodic monitoring of landslides by GPS, a geodetic deformation network capable of determining landslide motion is established at suitable places on hills to be monitored. Baselines between the network points are measured via GPS. GPS data are evaluated and the coordinates of each point are acquired. The differences in coordinates among the periods are addressed by deformation analysis. With this method, the movements of points can be determined, as well as the velocity and the direction of the movements (Bayrak 2003). This method is economical in terms of hardware and maintenance. Studies performed by Moss *et al.* (1999) and Gili *et al.* (2000) are examples of the monitoring of landslides.

In interpreting the deformations, mathematical and statistical techniques are utilized to identify relationships between deformations and their causes. Deformations, according to the surveying method and plan, are analyzed mainly by 3 models: static, kinematic, and dynamic (Ayan 1982; Acar *et al.* 2004). The static model is the most basic of these; using this approach determines only the geometric or local displacement of the object. When using the model, it is assumed that there is no motion of the object during the measurement belonging to a period (Ayan 1982; Acar *et al.* 2004). The kinematic deformation model involves the determination of the coordinates of the reference and the object points as functions of time (Pelzer 1985, 1987; Liu 1998). The dynamic deformation model determines,

* Correspondence: hastaoglukemal@gmail.com

in addition to the temporal behavior of the object, the variation of the forces causing deformation with respect to time, and the external factors and the functional relationship between these forces (Ayan 1982; Acar *et al*. 2004). Dynamic systems are affected by external forces and determine the system motions as a function of causal forces or the quantities proportional to these forces.

A variety of methods can be used to analyze deformations, such as the Kalman filtering technique. This is one of the most suitable prediction methods that can be applied to a dynamic system containing random errors. In this technique, analysis can be performed by modeling stochastic parameters belonging to periods and it is possible to model sudden changes in point positions (Demir 1999; Yalçınkaya & Bayrak 2003). Moreover, even if the number of the measurements is less than the number of unknown parameters, motion parameters can still be predicted depending on the suitable stochastic model chosen by the Kalman filter. It is considered that, if the stochastic models were established properly in all kinds of linear and nonlinear changes, this technique could be effective in determining deformations (Ünver & Öztürk 1994; Acar *et al*. 2004).

Many researchers have attempted to determine landslide deformations utilizing various deformation analysis methods (Önalp 1991; Altan *et al*. 1994; Dercourt 2000; Gili *et al*. 2000; Malet *et al*. 2002; Coe *et al*. 2003; Yalçınkaya & Bayrak 2003; Acar 2008). Most of these studies dealt with the time-dependent change in deformation amounts and obtained only the velocities belonging to landslide points (Önalp 1991; Altan *et al*. 1994; Acar 2008). It should be noted, however, that investigating only the time-dependent changes does not produce the necessary results for either the determination of factors causing landslides or the analysis of landslide mechanisms. Some researchers have attempted to determine the functions of forces, or the quantities related to these forces, that cause deformation by landslides by using the dynamic deformation model (Malet *et al*. 2002; Coe *et al*. 2003; Yalçınkaya 2003; Bayrak 2009).

Malet *et al.* (2002) determined seasonal and temporal flows in surface velocities by continuous monitoring of landslides via GPS measurements. They analyzed relationships between rainfall (and snowfall), groundwater level, and the displacements, and they determined the pore water pressure thresholds initiating an acceleration of the movement.

Coe *et al*. (2003) attempted to correlate the results obtained from hydrological and meteorological data with those obtained by GPS. Bayrak (2003) chose the variation in groundwater levels as the dynamic variable and generated a dynamic deformation model from position information obtained via GPS.

Coe *et al*. (2003) studied the Slumgullion landslide region in southwestern Colorado using extensometers and GPS for 3.5 years and determined the seasonal daily velocities. The velocities peaked in the first days of spring and in summer. When the temperature fell and the snowfall decreased in the middle of winter, the velocities slowed down. The authors showed that the variation in groundwater level changed the surface water seeping into the landslide material, and they emphasized the importance of continuous monitoring of surface water. They concluded that the variation in surface water is directly related to landslide velocities.

Bayrak (2003) chose Kutlugün village in the Cağlayan District of Trabzon (eastern Black Sea Region, Turkey) for his study. The variations in groundwater levels, which are the main cause of landslides in the region, were used as the dynamic variable in establishing the dynamic model. To determine the current borders of the landslide, a geodetic deformation network was established; 6 periods of GPS observations were carried out in the network at times determined according to the periods of minimum and maximum rainfall as shown by the meteorological data. At the same time, groundwater levels were measured by geological and geophysical observations. In order to obtain preliminary information in establishing the dynamic model, deformation analyses were carried out using the static and kinetic deformation models. Following this, dynamic deformation models were then established by taking into account the results of both above-mentioned models and groundwater levels. From the dynamic model results, it was concluded that variations in groundwater levels are very important in landslide occurrences.

In this study, the deformations were determined by using the Kalman filtering method as a function depending on temperature changes. Temperature variation was accepted as the indirect force causing deformations; snow melts due to the change in temperature, thus causing the groundwater level to increase. Both the landslides experienced in the region in 1998 and 2000 occurred in the periods when snow started to melt. The 6 periods of GPS data belonging to the landslide area, monitored by 2 fixed and 10 rover GPS points, were evaluated using Bernese V5.0 software; the deformation analyses were performed using kinematic and dynamic Kalman filtering. The velocities and accelerations with respect to time were obtained from the kinematic deformation analysis. According to the velocities obtained, an average annual movement of 8 cm was found at 1 point, whereas the velocities for other points ranged from 1 to 1.5 cm/year. The point at which the biggest movement was determined, namely KH07, was analyzed by the dynamic Kalman filtering method and the relationship between the amount of movement and temperature variation was defined. The Koyulhisar landslide area is shown in Figure 1. Hastaoglu

Figure 1. Landslide area (40°19′15″N, 37°50′09″E).

and Sanli (2011) determined only the velocities by regression analysis for the same GPS points. However, forces causing deformations were not investigated in their study. In this study, as distinct from that of Hastaoglu and Sanli (2011), the cause of the large motion of KH07 was examined. The relationship between the large motion of KH07 and the force causing deformation was modeled using the dynamic Kalman filtering technique.

2. Study area and GPS measurements

The study area is located in the north of the North Anatolian Fault Zone (NAFZ), a region affected by faulting. The main fault in the study area is the North Anatolian Fault, which extends in a NW–SE direction. The rocks outcropping in the landslide area consist of Pliocene volcanic, Eocene Yeşilce Formation, and limestones of the Maastrichtian age. These rocks are overlain by younger colluvium, essentially loose material detached from the bedrock masses by chemical, mechanical, and/or tectonic processes (Sendir & Yılmaz 2002).

The Koyulhisar District is located in a mountainous region. The Kelkit River, which is the most important and the biggest in the region, flows in an almost E–W direction, approximately parallel to the NAFZ. The highest hills and mountains are Boztepe, Saytepe, and Iğdır, with elevations of 1361, 1240, and 1850 m, respectively; the slope angles range from 20° to 75° (Sendir & Yılmaz 2002). A geologic map of the study area is shown in Figure 2 (Yilmaz 2009, p. 3, Fig. 2).

Koyulhisar is 180 km away from Sivas, Turkey. Since the study area lies upon the NAFZ, which is an active fault, the rock masses in the region contain discontinuities and are usually seen to be cracked and crushed. Depending on the steep topography in the region, there are many old and new landslides. The direction of motion of these landslides usually threatens residential areas (Sendir & Yılmaz 2002).

Koyulhisar is a region containing forests and high mountains. It is known that landslides have been encountered frequently in the region. Movements are usually observed after severe winters as debris flows mostly in the north of Koyulhisar. Furthermore, the landslides in 1998 and 2000 occurred after severe winter conditions (Sendir & Yılmaz 2002).

Huge and old landslide masses are seen in the Koyulhisar town center and in neighborhood areas where lower Miocene clay and gypsum levels, Eocene-aged clayey levels, and Plio-Quaternary terrace sediments exist. Most of these landslides have a mechanism involving a circular rotation. This old landslide mass is open-ended and it has maintained its activity. This activity is not related to the mass. These are local landslides that occur on the main mass (Tatar *et al.* 2000).

The deformations in the study area are local movements on the old landslide mass. This area is affected by tectonics due to the fact that it is on the NAFZ. As a result of tectonic effects, cracks occur in the area. Water that infiltrates through these cracks saturates the material. In the rainy seasons when the material becomes saturated the possibility of movement leading to landslides increases (Tatar *et al.* 2000).

The snow melting as a result of the temperature rise continues to flow underground towards Koyulhisar along the landslide area, especially in the Ufacık Puddle area, which is located 1 km away from the crown region of the Koyulhisar landslide (Figures 3 and 4).

The Kazan Puddle (Figure 5), which is about 5 m deep and covering 5000 m^2 in area, is formed by snow melting, especially between April and June every year, 25 m north of the old landslide area. According to local information, the Kazan Puddle forms between April and June and dries in July. It is estimated that snow water in the Kazan Puddle flows underground along the landslide area towards the Koyulhisar town center. Again, due to snow melting, a landslide puddle (Figure 4) of about 3 m in depth and covering 1500 m^2 forms on the landslide area. Similar to the Kazan Puddle, this puddle fills between April and June and dries in July. As may be understood from the patterns of formation of these puddles, the level of underground water increases by snow melt when the weather becomes warmer, between April and June (Figure 6).

By studying the regional meteorological data it may be seen that the temperature rises between April and May, peaks during August, and starts to decrease from October to November. Rainfall is at its maximum level between April and May (Figure 6) and at its minimum during August; it increases again between October and November. In consideration of these periodic changes, both in the temperature and the rainfall, April, August, and November were chosen as GPS measurement periods. In order to detect slides in the study area, 2 reference and 10 rover GPS points were established. A total of 5 points (2 on the top of the landslide (KH01 and KH02), 2 on the landslide mass (KH03 and KH04), and 1 on a pillar (KH05)), were

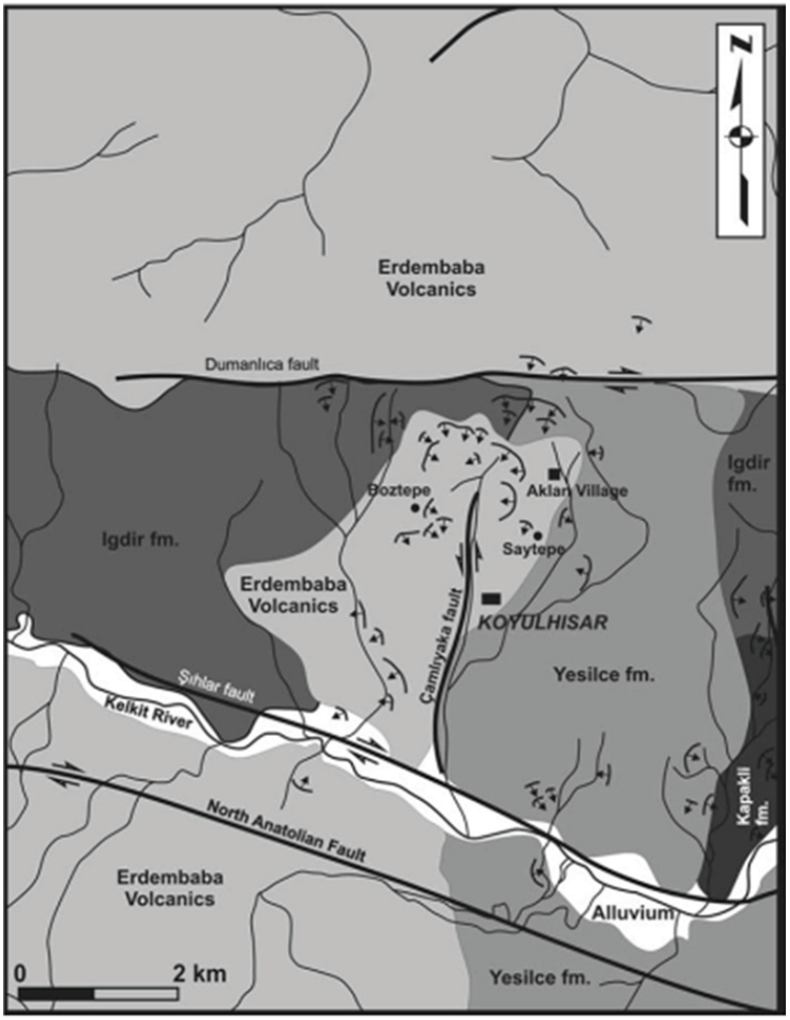

Figure 2. Geologic map of the project area (from Yilmaz 2009).

Figure 3. Ufacık Puddle Region, April 2007 (40°20′19″N, 37°50′07″E).

Figure 4. Some puddles occur in the Koyulhisar landslide area, April 2007 (40°19′20″N, 37°50′14″E).

Figure 5. Kazan Puddle, April 2007 (40°20′18″N, 37°50′08″E).

placed within the former landslide area to assess the current situation of the landslides that occurred in 1998 and 2000. Moreover, to determine the current situation in the county, 5 more GPS points were established: 2 in the north of the district (KH06, KH11), 2 in the center of the district (KH07, KH10), and 1 in the south of the district. A total of 6 periods of GPS measurements were performed at 12 points between 2006 and 2008. Each GPS campaign was carried out on 3 consecutive days; each observation session regarding the static GPS measurements lasted about 12 h. GPS data were evaluated using Bernese V5.0 software, and the coordinates were obtained from each period from these 12 points. GPS points are given in Figure 7.

3. Determination of velocity and acceleration of GPS points using kinematic Kalman filter

Movement was then assessed using static and kinematic models. Only points that moved and movement quantities were determined using the static model. In addition to the point positions, the velocities and accelerations at these positions were also determined utilizing the kinematic model's time-dependent function, using the Kalman filter technique (Yalçınkaya 2003).

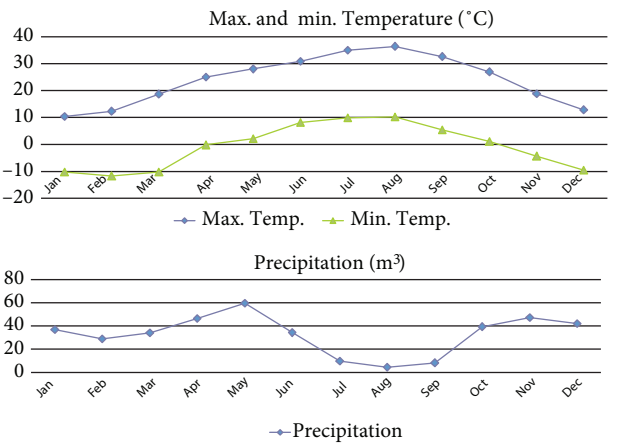

Figure 6. Average temperature and precipitation values of Koyulhisar.

The purpose of kinematic models is to find a suitable description of point movements by time functions without regarding potential relationships with causative forces. Polynomial approaches, especially velocities and accelerations, and harmonic functions are commonly applied (Welsch & Heunecke 2001).

The Kalman filtering method is used in the prediction of state vector information in motion parameters known in t_{i-1} period and of the state vector by the help of measurements done at period t_i. A motion model comprising position, velocity and acceleration is given in Eq. (1).

$$n_j^{(k+1)} = n_j^{(k)} + (t_{k+1} - t_k)v_{nj} + \frac{1}{2}(t_{k+1} - t_k)^2 a_{nj}$$

$$e_j^{(k+1)} = e_j^{(k)} + (t_{k+1} - t_k)v_{ej} + \frac{1}{2}(t_{k+1} - t_k)^2 a_{ej}$$

$$up_j^{(k+1)} = up_j^{(k)} + (t_{k+1} - t_k)v_{upj} + \frac{1}{2}(t_{k+1} - t_k)^2 a_{upj} \quad (1)$$

$n_j^{(k)}, e_j^{(k)}, up_j^{(k)}$: coordinate of point j at time (t_k) period.

v_{nj}, v_{ej}, v_{upj} : velocities of n, e, up coordinates of point j.

a_{nj}, a_{ej}, a_{upj} : accelerations of n, e, and up coordinates of point j, k = 1,2, …,i (i: measurement period number), j = 1,2, ….,n (n number of points).

The Kalman filtering method is composed of 3 main phases: prediction, filtering, and smoothing (Cross 1990). In Eq. (1), unknown motion parameters consist of position and velocity as the first derivative of position as well as acceleration, which is the second derivative of position. To compute the motion parameters of points with the Kalman filtering technique, the matrix form of position, velocity, and acceleration can be written as in Eq. (2).

$$\bar{Y}_{k+1} = \begin{bmatrix} n \\ e \\ up \\ v_n \\ v_e \\ v_{up} \\ a_n \\ a_e \\ a_{up} \end{bmatrix}_{k+1} = \begin{bmatrix} I & I(t_{k+1} - t_k) & I\frac{(t_{k+1} - t_k)^2}{2} \\ 0 & I & I(t_{k+1} - t_k) \\ 0 & 0 & I \end{bmatrix}_{k+1,k} \begin{bmatrix} n \\ e \\ up \\ v_n \\ v_e \\ v_{up} \\ a_n \\ a_e \\ a_{up} \end{bmatrix}_k \quad (2)$$

Eq. (2) can be written in a shorter form as

$$\bar{Y}_{k+1} = T_{k+1,k}\hat{Y}_k \quad (3)$$

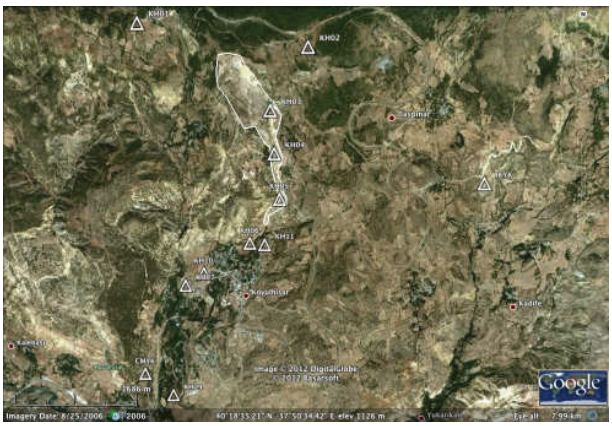

Figure 7. Location of GPS points utilized in the study (courtesy of Google Earth™).

where $\bar{Y}_{k+1}$ is the status vector at time t_{k+1}, $\hat{Y}_k$ the status vector at time t_k, $T_{k+1,k}$ is the prediction matrix, and I is the unit matrix. Eq. (3) is the fundamental Kalman filtering equation. System noises in the prediction equation are considered as S noise vector composed of the values at the last column of the $T_{k+1,k}$ matrix in Eq. (3) as w is constant acceleration between periods t_{k+1} and t_k. As a consequence, prediction and covariance matrices would be as follows (Gülal 1999; Acar *et al*. 2008; Bayrak 2009).

$$\bar{Y}_{k+1} = T_{k+1,k}\hat{Y}_k + S_{k+1,k}\,w_k \tag{4}$$

$$Q_{\bar{Y}\bar{Y},k+1} = T_{k+1,k}\,Q_{\hat{Y}\hat{Y},k}\,T^T_{k+1,k} + S_{k+1,k}Q_{ww,k}S^T_{k+1,k} \tag{5}$$

$$S^T_{k+1,k} = \left[I\frac{(t_{k+1}-t_k)^2}{2} I(t_{k+1}-t_k)I \right] \tag{6}$$

The system noise is considered as the noise matrix S (random errors of the model) that consists of the terms of the last column of the T prediction matrix. $S_{k+1,k}$ is the random noise vector between periods t_{k+1} and t_k and is composed of the values at the last column of the $T_{k+1,k}$ matrix in Eq. (3), $Q_{\hat{Y}\hat{Y},k}$ is the cofactor matrix of status vector at time t_k, and $Q_{ww,k}$ is the cofactor matrix of system noises at time t_k.

The acceleration vector of effects w is indefinite and as a rule cannot be measured. Thus, the pseudo-observation vector can be taken as w = 0 (Bayrak 2009). The adjustment of the problem can be expressed in matrix form as:

$$l_{k+1} + v_{l,k+1} = A_{k+1}\hat{Y}_{k+1} \tag{7}$$

where I_{k+1} are the measurements at time t_{k+1}, $V_{l,k+1}$ are residuals, A_{k+1} is the coefficients matrix, and $\hat{Y}_{k+1}$ are measurements in period k+1. The functional and stochastic models for the Kalman filter techniques combining Eq. (4) and (7) can be written in matrix form (Yalçınkaya & Bayrak 2005; Acar *et al*. 2008; Bayrak 2009) as:

$$\begin{bmatrix} \bar{Y}_{k+1} \\ l_{k+1} \end{bmatrix} = \begin{bmatrix} I \\ A_{k+1} \end{bmatrix} \hat{Y}_{k+1} - \begin{bmatrix} v_{\bar{Y},k+1} \\ v_{l,k+1} \end{bmatrix}; Q_i = \begin{bmatrix} Q_{\bar{Y}\bar{Y},k+1} & 0 \\ 0 & Q_{ll,k+1} \end{bmatrix} \tag{8}$$

The model is solved and movement parameters and their cofactor matrix are computed.

In this study, the 6 periods of GPS measurements for the 10 GPS points within the landslide area were evaluated by Bernese V5.0 software, and their coordinates were computed. Using the 3D kinematic Kalman filtering model generated by using obtained coordinates and given in Eq. (1), the velocity and acceleration values were predicted for the GPS points. This was then tested using the Student t-test, setting the significance level at α = 0.05 to determine whether the results were statistically significant. Statistical tests of the expanded model were conducted, and it was decided that the model consisting of velocity and acceleration was significant (Table 1). Every parameter (velocity and acceleration) was divided by its root mean square error, and test values were computed. Statistical tests were conducted as mentioned previously and results are shown in the decision column of Table 1. If parameters have significantly changed in the kinematic model, a "√" sign is given in Table 1. Otherwise, a "–" sign is given. Hastaoglu and Sanli (2011) determined only the velocities by regression analysis for the same points. The velocities predicted by the Kalman filtering method in this study are highly compatible with those found by Hastaoglu and Sanli (2011). The predicted velocity and acceleration values in the current study are given in Table 1, where it can be seen that the velocity values of v_{nKH3}, v_{eKH5}, v_{nKH6}, v_{nKH7}, v_{eKH7}, and v_{eKH9} and the acceleration values of a_{nKH3}, a_{eKH5}, a_{nKH7}, and a_{eKH7} are significant. While the velocities for points KH03, KH06, and KH09 are about 1–1.5 cm/year, the north and east components of KH07 are 6.44 and 4.78 cm/year, respectively. Point KH07, in the southwestern end of the landslide area, moves horizontally about 8 cm/year. This movement was confirmed by photos taken during the field work (Figure 8).

All velocity values associated with these points were determined by the Kalman filtering method, and the values are presented in Table 1 and Figure 9. As shown in Table 1, an average movement of 1.5 cm/year was seen at the points on the former landslide mass, whereas a movement of 8 cm/year was observed at point KH07 in the center of the district. In conclusion, although 10 GPS points were established in the region, a slide of more than 2 cm was only determined at point KH07. As Sendir and Yılmaz (2002) stated, a number of landslides having complex structures and taking N–S directions are present in the region. Some deformations were observed, especially concerning buildings, in the vicinity of KH07. Information obtained either from the local community or

Table 1. Movement parameters determined with the kinematic model between April 2007 and September 2008.

	Velocity unknowns (cm/year)			Decision			Acceleration unknowns (cm/year^2)			Decision		
Point	v_n	v_e	v_{up}	dv_n	dv_e	dv_{up}	a_n	a_e	a_{up}	da_n	da_e	da_{up}
KH01	0.23	−0.36	−0.34	0.25(−)	0.50(−)	0.27(−)	0.16	−0.16	−0.09	0.17(−)	0.18(−)	0.09(−)
KH02	0.99	−0.38	−0.07	1.24(−)	0.71(−)	0.06(−)	0.49	−0.34	−0.11	0.58(−)	0.46(−)	0.12(−)
KH03	1.18	−0.34	−0.42	**2.65**(√)	0.45(−)	0.38(−)	1.91	−0.31	−0.06	**3.12**(√)	0.36(−)	0.07(−)
KH04	−0.31	−0.15	−1.11	0.50(−)	0.25(−)	0.93(−)	−0.12	−0.02	−0.22	0.15(−)	0.02(−)	0.23(−)
KH05	0.04	−1.46	0.00	0.04(−)	**2.76**(√)	0.01(−)	−0.02	−1.55	0.02	0.02(−)	**2.00**(√)	0.02(−)
KH06	−1.57	0.15	1.01	**1.85**(√)	0.22(−)	1.08(−)	−0.50	0.08	−0.13	0.55(−)	0.10(−)	0.14(−)
KH07	−6.44	−4.78	−0.25	**9.72**(√)	**5.02**(√)	0.20(−)	−1.78	−1.89	−0.27	**2.09**(√)	**2.17**(√)	0.28(−)
KH09	−0.35	−1.45	0.29	0.41(−)	**1.71**(√)	0.28(−)	−0.15	−0.97	−0.21	0.17(−)	1.15(−)	0.23(−)
KH10	0.36	−0.35	0.31	0.49(−)	0.35(−)	0.44(−)	0.21	−0.19	0.14	0.24(−)	0.21(−)	0.17(−)
KH11	0.14	−1.49	−0.06	0.37(−)	1.53(−)	0.07(−)	0.15	−0.55	0.05	0.23(−)	0.61(−)	0.06(−)

other authorities indicates that there are visible landslides around KH07, but there are no other visible landslides in the region. This shows that the landslides identified in this study by GPS observations concur with the information supplied by the local community and other authorities.

Even though there are no hydrological data available for the period between 2006 and 2009, a hole was drilled in the basement of the Police Department, which is located 15 m away from point KH07 (Figure 10). Water is available in this drill hole at a depth of 20 cm and is being drained continuously. According to information obtained from the Police Department, the water level increases especially in the spring season and decreases in the summer. It is reasonable to ascribe the large motion at KH07 to the ground water level

4. Determination of the relationship between temperature and displacement by using the dynamic Kalman filter

In fact, the main factor is the wet winter season before the landslide occurrence. In winter the slopes are covered with a thick snow pack, which slowly melts in the spring and the slope becomes saturated. The saturation of the earth on the slope causes a rise in water pressure, the shear strength (resisting forces) decreases, and the weight (driving forces) increases. The net effect is to lower the safety factor. In the toe of both landslides, springs from the infiltrated water were observed (Sendir & Yılmaz, 2002).

Ulusay *et al.* (2007) noted that, in this region, although there is no information on the thickness of the snow cover in the landslide source area before the event, the period between March and May generally corresponds to the snow melting period. Snow melts therefore seem to be more important than rainfall in precipitating a landslide event. Site observations and back-analysis of the initial slide suggest that the most likely cause is probably water pressure increase, as it is the season of snow melts and the thawing of the groundwater.

Tatar *et al.* (2000) suggested that some deformations are observed around KH07 and these deformations are due to local landslides in the main mass. The main cause of local landslides is that the water infiltrate from these crack systems saturates the material. Ulusay *et al.* (2007) pointed out that melting snow is more effective than rain in increasing groundwater. Previous landslides in the region have occurred after snow has melted in the summer season, when the amount of rain is at the minimum level. Consequently, the main factor that affects landslides is that of snow melting, which increases the water level and makes the material water saturated. Snow melts from March, when the temperature is beginning to increase, to June, when the temperature becomes stable

Briefly, when the horizontal deformation of KH07 is examined (Figures 11 and 12), it is observed that the movement increases as the temperature increases between March and June. The movement decreases when the temperature decreases and it begins to snow.

The kinematic Kalman filtering method was applied to data related to all points on the landslide. It was then decided that a dynamic model should be applied again for all points. Charts (Figure 11) that show displacement depending on the times of KH03, KH05, and KH07 that have significant acceleration and velocity values as a result of kinematic Kalman filtering were examined in order to decide on the dynamic model to be applied. When these charts were examined, no systematic change was observed for KH03 and KH05, whereas a systematic change dependent on time and season was observed for

Figure 8. The deformation near KH07 caused fractures and cracks in the buildings and on the ground (40°18′06″N, 37°49′30″E).

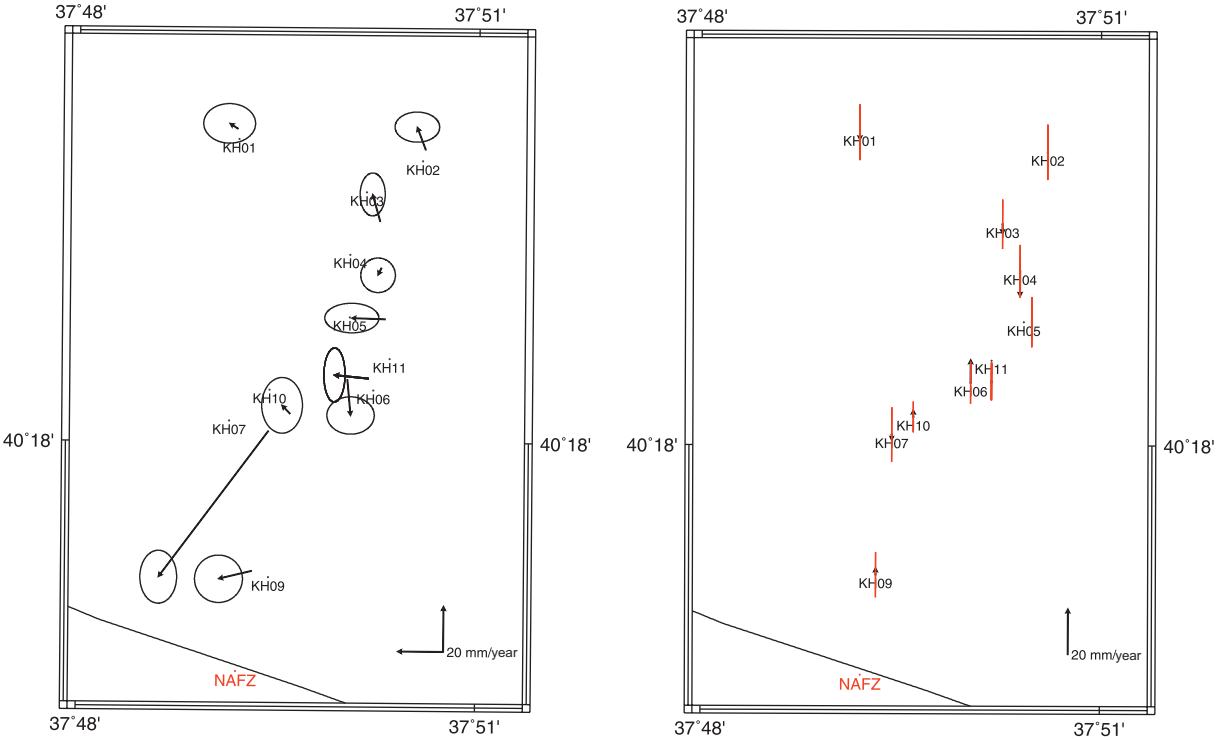

Figure 9. Horizontal and vertical velocity field (left: horizontal velocities; right: vertical velocities). NAFZ = North Anatolian Fault Zone.

Figure 10. Pictures of drill hole in the basement of the Police Department, located 15 m away from point KH07 (40°18′05″N, 37°49′26″E).

KH07. This change is described by Eq. (9). Although the seasonal effect was not observed on the charts of displacement of KH03 and KH05, a dynamic model was applied to all points on the landslide. As a result of this process, a significant movement was identified only at KH07; insignificant movements were determined at other points. Coefficients depending on temperature change were therefore estimated only for KH07.

A different motion was observed at KH07, as can be seen from the values provided in Table 1. These values indicate that no significant motion was observed for the elevation component of KH07, whereas a motion of 8 cm/year in the horizontal components was observed. Figure 12 clearly shows that the motion slows down in the summer season; the figure also suggests that the motion accelerates from October to April and from April to July. Thus, a seasonal effect can be suggested for point KH07.

Figure 12 shows an observed increase in the magnitude of displacements at KH07, especially when the temperature begins to rise and, together with the

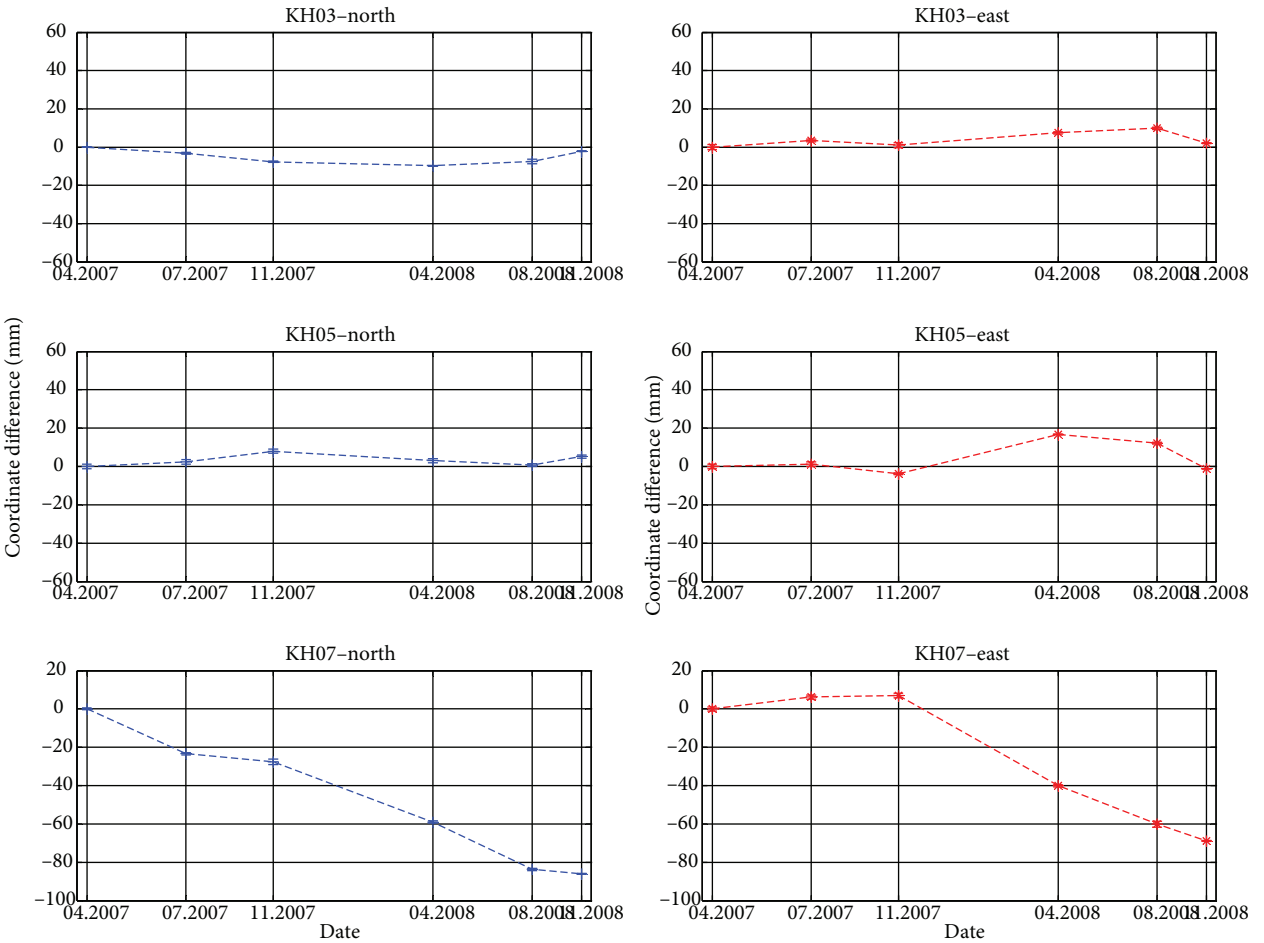

Figure 11. Coordinate differences of KH03, KH05, and KH07.

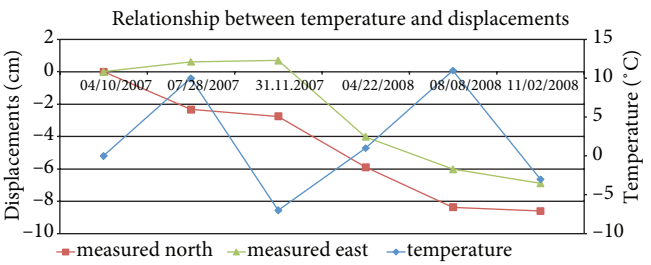

Figure 12. Temperature–displacement relationship for north and east components of point KH07.

decrease in temperature, the displacement becomes steady. There is high snowfall in the region between November and February. Snow accumulates in this region (the Ufacık Puddle Region), which is located in the north of the landslide area. Together with the rise of average temperature of over 10 °C in April, the snow accumulated in the Ufacık Puddle Region begins to melt and seep underground, producing an increase in groundwater level.

In order to show the relationship between groundwater and the displacement of point KH07, a dynamic model was generated using the data that originated from the northern and eastern components of point KH07. In the $x = f(t, \Delta S)$ dynamic model, ΔS denotes the temperature difference between the periods. The 2D position vector composed of the northern and eastern components of KH07 and the motion model composed of the external force (temperature) generated according to the dynamic Kalman filtering method are given in Eq. (9).

$$n_j^{(k+1)} = n_j^{(k)} - e^{(S_{k+1}-S_k)/10} s_{nj}$$
$$e_j^{(k+1)} = e_j^{(k)} - e^{(S_{k+1}-S_k)/10} s_{ej} \quad (9)$$

Here, $n_j^{(k+1)}$ and $e_j^{(k+1)}$ are the coordinates of point j at time (t_{k+1}), $S_{nj}^{(k)}$ and $S_{ej}^{(k)}$ are the coordinates of point j at time (t_{k+1}), and are temperature parameters of n and e coordinates of point j, S_{k+1} is the temperature value at time (t_{k+1}), and S_k is the temperature value at time (t_k).

To compute the motion parameters of points with the dynamic Kalman filter technique, the matrix form of position and temperature for KH07 can be written as follows.

$$\bar{Y}_{k+1} = \begin{bmatrix} n \\ e \\ s_n \\ s_e \end{bmatrix}_{k+1} = \begin{bmatrix} I & I(-e^{(s_{k+1}-s_k)/10}) \\ 0 & I \end{bmatrix}_{k+1,k} \begin{bmatrix} n \\ e \\ s_n \\ s_e \end{bmatrix}_k \quad (10)$$

Eq. (10) is the prediction equation. The model is solved according to the Kalman filter solution, and 2D displacements and temperature parameters are computed. The predicted temperature parameters are given in Table 2.

The results obtained from the dynamic and kinematic models of point KH07 are given in Figure 13. Figures 13a and 13b and Table 3 provide the measurement, prediction, and filtering results obtained from the dynamic and kinematic models for the northern component of KH07. As can be seen, the prediction and filtering results obtained by the dynamic model for the northern component are more consistent and compatible with the measured values. The dynamic model, which takes the effect of temperature into account for the northern component, produced more consistent values compared to the kinematic model.

Figures 13c and 13d and Table 3 present the measured, predicted, and filtering results obtained from the dynamic and kinematic models for the eastern component of KH07. It can be seen that the prediction and filtering results, especially those obtained after the third period from the dynamic model, are close to the measured values. For the motion of KH07, the dynamic model prediction values are more compatible with the measured values.

Table 4 presents the coefficient of determination R^2 and the correlation values between the measured values and the prediction and filtering values obtained from the dynamic and kinematic models. R^2 is the square of the correlation coefficient. R^2 gives the proportion of sample variety in a dependent variable that is explained by the independent variable (temperature). As shown in Table 4, the correlation values of the dynamic model are more appropriate than those of the kinematic model.

5. Conclusions

This paper describes the modeling of relationships between displacements and groundwater based on a new dynamic analysis method developed for the large motion of KH07. This analysis models and identifies how the temperature triggers the large motion of KH07 during high temperature periods through ground water level changes. In this study, the velocity and acceleration values were determined according to the kinematic analysis method for 10 GPS points in the Koyulhisar landslide. As a result of kinematic analysis, velocity or acceleration values were determined as significant for 5 of these 10 points. For only 3 of these 5 points, both the velocity and acceleration values were significant, whereas only the velocity values were significant for 2 points. Average annual velocities were measured at about 1.5 cm for 4 of the 5 points, but at 8 cm at 1 point. Accordingly, it was considered that the displacement mechanism for this point differs from the mechanism of the others and the reasons for this were investigated. Furthermore, it was also considered that there might be a relationship between the displacements belonging to the periods of groundwater variation, and so a dynamic model, which can reflect the relationship between the displacements and temperature, was established for KH07. By means of this new dynamic analysis model, the horizontal components of the coordinates of point KH07 were analyzed using the Kalman filtering technique. Thus, the relationship between temperature and displacement was assessed mathematically.

Table 2. Results of dynamic model for temperature parameters s_n and s_e.

Epochs	Temperature parameter (cm)		Decision	
	s_n	s_e	ds_n	ds_e
Jul.07–Apr.07	1.412	1.445	14.68(√)	14.17(√)
Dec.07–Apr.07	1.408	1.421	14.15(√)	13.57(√)
Apr.08–Apr.07	1.384	1.420	14.97(√)	14.11(√)
Aug.07–Apr.07	–0.283	–0.298	16.47(√)	13.78(√)
Dec.08–Apr. 07	–0.282	–0.299	9.91(√)	9.60(√)

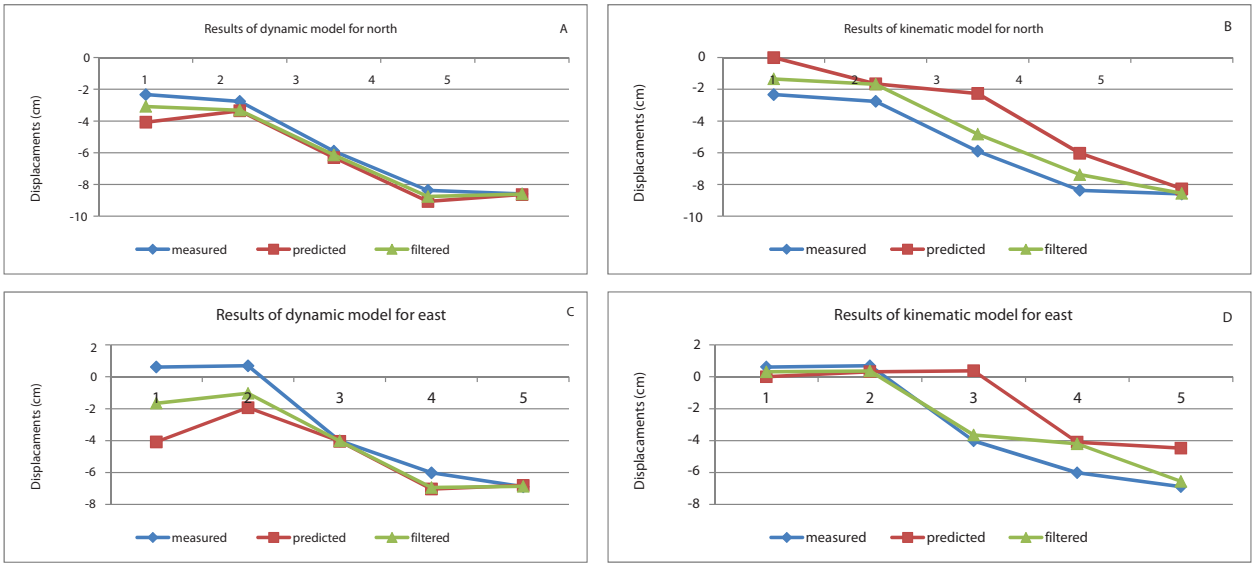

Figure 13. Measured, predicted, and filtered values of KH07 by using dynamic and kinematic models.

Table 3. Values of measured, filtered, and predicted displacements.

	North component (cm)					East component (cm)				
Date	Measurement	Dynamic		Kinematic		Measurement	Dynamic		Kinematic	
		Filtered	Predicted	Filtered	Predicted		Filtered	Predicted	Filtered	Predicted
Jul.07	–2.3	–3.1	–4.1	–1.3	0.0	0.6	–1.7	–4.1	0.3	0.0
Nov.07	–2.8	–3.3	–3.4	–1.7	–1.7	0.7	–1.0	–1.9	0.4	0.3
Apr.08	–5.9	–6.1	–6.3	–4.8	–2.3	–4.0	–4.0	–4.0	–3.6	0.4
Aug.08	–8.4	–8.8	–9.1	–7.4	–6.0	–6.0	–6.9	–7.0	–4.2	–4.1
Nov.08	–8.6	–8.6	–8.6	–8.6	–8.3	–6.9	–6.9	–6.8	–6.6	–4.5

Table 4. Correlation and coefficient of determination values between measured and filtered and predicted displacements.

	North component				East component			
	Dynamic		Kinematic		Dynamic		Kinematic	
	Filtered	Predicted	Filtered	Predicted	Filtered	Predicted	Filtered	Predicted
Correlation (c)	0.998	0.983	0.993	0.928	0.981	0.875	0.980	0.827
Coefficient of determination (R^2)	0.996	0.967	0.987	0.862	0.963	0.766	0.961	0.684

The predicted and filtered displacements obtained for each observation period by kinematic and dynamic Kalman filtering were compared. As a result of this comparison it was observed that the predicted displacements, especially those obtained from the dynamic model, are more consistent with the real values. This result suggests that the dynamic model may give more suitable results for future predictions related to the motion of KH07. The results also revealed that groundwater and meteorological data need to be collected at GPS stations. Hence, direct correlation of groundwater data with the land motion will be possible, and an improved dynamic model with ground motion data will lead to better future predictions.

Acknowledgments
The author thanks the project's members and also officials and local people in the region for their help. Ercüment Ayazlı, Fatih Poyraz, and Önder Gürsoy are acknowledged for their support with GPS data collection and monumentation, respectively. BERNESE 5.0 was provided for GPS data processing by TÜBİTAK MAM under a contract through a State Planning Organization (SPO) project with Grant 2006 K-120220. Some of the GPS campaigns were also funded by the SPO project. Cumhuriyet University funded the Koyulhisar Landslide Project with Grant M-330. Google Earth was used to draw the map of the Koyulhisar landslide. GMT was used to draw the velocity map of the Koyulhisar landslide. TÜBİTAK Funded the Koyulhisar Landslide project with Grant 111Y111.

References

Acar, M., Ozludemir, T., Erol, S., Celik, R.N. & Ayan, T. 2004. Landslide monitoring through Kalman filtering: A case study in Gürpınar. *ISPRS* July 2004, İstanbul, Turkey.

Acar, M., Ozludemir, T., Erol, S., Celik, R.N. & Ayan, T. 2008. Kinematic landslide monitoring with Kalman filtering. *Natural Hazards and Earth System Sciences* **8**, 213–221.

Altan, M.O., Ayan, T., Deniz, R., Tekin, E. & Özüer, B. 1994. Determination of soil movements at a landslide area. *Proceedings of 1st Turkish International Symposium on Deformations*, İstanbul, Turkey, 692–699.

Ayan, T. 1982. An overview of deformation analysis on geodetic networks. *Journal of Istanbul Technical University* **1**, 40 (in Turkish).

Bayrak, T. 2003. Developing a dynamic deformation model and a dynamic movement surface model for landslides. PhD, Karadeniz Technical University, Graduate School of Natural and Applied Sciences, Trabzon, Turkey (in Turkish).

Bayrak, T. 2009. Determining the influence of rainfall on the activity of Kulugun landslide. *Fresenius Environmental Bulletin*, **18**, 7b.

Brunner, F.K. 1997. Continuous monitoring of deformation using the Global Positioning System. *AvH Magazine* **69**, 29–38.

Brunner, F.K. & Welsch, W.M. 1993. Effects of the troposphere on GPS measurements. *GPS World* **4**, 42–51.

Coe, J.A., Ellis, W.L., Godt, J.W., Savage, W.Z., Savage, J.E., Michael, J.A., Kibler, J.D., Powers, P.S., Lidke, D.J. & Debray, S. 2003. Seasonal movement of the Slumgullion landslide determined from Global Positioning System surveys and field instrumentation, July 1998–March 2002. *Engineering Geology* **68**, 67–101.

Cross, P.A. 1990. Advanced Least Squares Applied to Position Fixing. Working Papers. North East London Polytechnic, Department of Surveying.

Demir, C. 1999. Investigation of horizontal crustal deformation and strain on the west part of the North Anatolion Fault Zone. PhD, Yıldız Technical University, Graduate School of Natural and Applied Sciences, İstanbul.

Dercourt, J. 2000. Apport du GPS au Suivi en Continu des Mouvements de Terrrain: Application au Glissement-Coulee de Super-Sauze (Alpes-de-Haute-Provence,France). *Earth and Planetary Sciences* **331**, 175–182 (in French with English abstract).

Gili, J.A., Corominas, J. & Rius, J. 2000. Using Global Positioning System techniques in landslide monitoring. *Engineering Geology* **55**, 167–192.

Gülal, E. 1999. Kalman filtreleme tekniğinin deformasyon ölçülerinin analizinde uygulanması. *Journal of Yıldız Technical University* **1**, 10–19 (in Turkish).

Hastaoglu, K. & Sanli, D.U. 2011. Monitoring Koyulhisar landslide using rapid static GPS: a strategy to remove biases from vertical velocities. *Natural Hazards* **58**, 1275–1294.

Liu, Q. 1998. Geodetic models of crustal deformation and their applications to the determination of recent crustal deformation and strain accumulation in the DTYG area inferred from terrestrial and GPS measurements. PhD, Helsinki University of Technology, Department of Surveying.

Malet, J.P., Maquaire, O. & Calais, E. 2002. The use of Global Positioning System techniques for the continuous monitoring of landslides: application to the Super-Sauze Earthflow (Alpes-de-Haute-Provence, France). *Geomorphology* **43**, 33–54.

Moss, J.L., McGuire, W.J. & Page, D. 1999. Ground deformation of a potential landslide at La Palma, Canary Islands. *Journal of Volcanology and Geothermal Research* **94**, 251–256.

Önalp, A. 1991 Doğu Karadeniz Bölgesi Heyelanları - Nedenleri Analizi ve Kontrolü. Proc. K.T.Ü Türkiye *1. Heyelan Sempozyumu Bildiriler Kitabı*, 85–86 (in Turkish).

Pelzer, H. 1986. Application of Kalman- and Wiener-filtering on the determination of vertical movements. *The Symposium on Height Determination on Recent Vertical Crustal Movements in Western Europe*, Hannover, 539–555.

Pelzer, H. 1987. Deformationsuntersuchungen auf der Basis Kinematischer Bewegungungsmodelle. *AVN 94* **2**, 49–62 (in German).

Sendir, H. & Yılmaz, I. 2002. Structural, geomorphological and geomechanical aspects of the Koyulhisar landslides in the North Anatolian Fault Zone (Sivas, Turkey). *Environmental Geology* **42**, 52–60.

Tatar, O., Aykanat, D., Kocbulut, F., Yilmaz, I., Sendir, H., Kurcer, A. & Saglam, B. 2000. Landslide Investigation and Assessment Report of Koyulhisar Town Centre and District Police Chief Building. Faculty of Engineering, Cumhuriyet University, Sivas, Turkey (in Turkish).

Ulusay, R., Aydan, Ö. & Kilic, R. 2007. Geotechnical assessment of the 2005 Kuzulu

landslide (Turkey). *Engineering Geology* **89**, 112–128.

Ünver, M. & Öztürk, E. 1994. Determination of vertical crustal movement. *Proceedings of 1st International Symposium on Deformation*, İstanbul, 303–314.

Welsch, W.M. & Heunecke, O. 2001. Models and terminology for the analysis of geodetic monitoring observations. *Proceedings of the 10th International Symposium on Deformation Measurements*, Orange, CA, USA, 390–412.

Yalçınkaya, M. 2003. Monitoring crustal movements in West Anatolia by precision leveling. *Journal of Surveying Engineering*, **129**, 44–49.

Yalçınkaya, M. & Bayrak, T. 2003. Dynamic model for monitoring landslides with emphasis on underground water in Trabzon province. *Journal of Surveying Engineering* **129**, 115–124.

Yalçınkaya, M. & Bayrak, T. 2005. Comparison of static, kinematic and dynamic geodetic deformation models for Kutlugün landslide in Northeastern Turkey. *Natural Hazards* **34**, 91–110.

Yilmaz, I. 2009. A case study from Koyulhisar (Sivas-Turkey) for landslide susceptibility mapping by artificial neural networks. *Bulletin of Engineering Geology and the Environment* **68**, 297–306.